Purdue University
Purdue e-Pubs

International Refrigeration and Air Conditioning Conference

School of Mechanical Engineering

1996

Vapor-Liquid Equilibria in R23/R1 16 System and Its Thermodynamic Properties

V. P. Zhelezny
Odessa State Academy of Refrigeration

Y. V. Semenyuk
Odessa State Academy of Refrigeration

V. N. Anisimov
Odessa State Academy of Refrigeration

Follow this and additional works at: http://docs.lib.purdue.edu/iracc

VAPOR - LIQUID EQUILIBRIA IN R23/R116 SYSTEM AND ITS THERMODYNAMIC PROPERTIES

V. P. Zhelezny,   Yu. V. Semenyuk,   V. N. Anisimov

Thermophysical Engineering Department
Odessa State Academy of Refrigeration
Petra Velikogo Street 1/3, Odessa, 270100, Ukraine
phone (0482) 68 13 90, fax (0482) 23 89 31

Abstract

Vapor - liquid equilibria and PVTx properties of binary refrigerant mixture R23/R116 have been measured by means of a variable volume method. The measurements were performed at compositions of 10.15, 22.32, 36.00, 47.36, 56.24, 70.10 and 87.67 mol. % R116. The uncertainties of the temperature, pressure and density measurements were estimated to be not greater than 15mK, 0.3% and 0.3% respectively. Also the critical parameters (T_c, P_c and ρ_c) for this mixture have been measured. The parameters of the cubic equation of state calculated from our measurements are presented too.

Nomenclature

K_{ij} — binary interaction parameter

P — pressure, MPa

R — $= 8.3145 \cdot 10^{-3}$, universal gas constant, kJ(molK)$^{-1}$

T — temperature, K

V — molar volume, m^3 mol^{-1}

X — mole fraction of R116

ρ — density, kg m^{-3}

τ — $= T/T_c$, reduced temperature

Introduction

The binary system R23/R116 may be suitable replacement for the refrigerants R13 and R503 wich are widely used as working fluids in refrigerant equipment. The aim of this work is to present experimental vapor-liquid equilibria (VLE) and PVTx data and provide parameters for the cubic equation of state for this mixture.

Experimental

The experimental apparatus is shown schematically in Fig. The main part of the apparatus is an optical cell (A). The body of this cell was made of the molybdenum glass (300 mm long, 3.4 and 9.6 mm in inner diameters). The inner volume calibrated by using mercury is about 14 cubic cm . The optical cell was installed in a thermostatic bath (I) with heat-transfer medium that was circulated by stirrer (D). The temperature measurement was made by calibrated 10 ohm platinum resistance thermometer (G) (Model PTS-10) with the aid of potentiometer (O) (Model R348). The thermometer was placed in the vicinity of the optical cell. In order to keep the temperature constant

another 100ohm platinum resistance thermometer (F) was mounted into the thermostated bath.The temperature fluctuation was detected by thermometer (F) and temperature control was carried out by the 1 kW main heater (C), 40 W subheater (E), thermometer bridge (M) (Model MO-62), PID controller (L) (Model VRT-2) and thyristor amplifier (K). The pressure inside the balloon (Q) had been transmitted to mercury and to oil through a visual separators (R). The dead-weight pressure gauge (P) (Model MP-60) was directly used to measure the pressure. The level of mercury and vapor-liquid interface was determined by visual observation. The sample density was calculated from the inner volume of the cell and the mass of the confined mixture. The composition of the mixture was determined by weighting the mass of each pure components before mixing.

PVTx properties were measured on the isotherms.

Determination of the saturation state of a mixture with a prescribed composition was performed by observing the appearance of a bubble in the liquid-phase sample confined in the cell.

The parameters on the dew curve were determined in the points, where isotherms of gaseous phase crossed the isotherms of double-phase region. For analysis of the results of measurements near the dew curve a method of investigation the PVT properties in the region of blurred phase transition considered in [1] was used.

The critical point was determined by observing disappearance and reappearance of the meniscus.

The purities of each component supplied was 99.79% R23 and 99.80% R116. The experimental uncertainty in determining the concentration was estimated as 0.0008 mol/mol, temperature - at 15 mK. Taking into account the systematic and accidental errors, full error in pressure value was equal to 0.1-0.3% in all pressure region,the one of liquid density was about 0.2-0.3%, for vapor density - 0.15-0.25%. The uncertainties in the critical temperature, critical pressure and critical density have been estimated to be within 20 mK, 8 kPa and 6 kg/m^3, respectively.

Results

The measurements were performed at compositions of x: 0.1015; 0.2232; 0.3600; 0.4736; 0.5624; 0.7010; and 0.8767 mol/mol R116 in the following ranges: for temperature from 243.15 to 298.15 K, for pressure from 1.0 to 3.4 MPa and for density from 50 to 250 kg/m^3 in the vapor phase. In addition, the bubble-point pressures and saturated-liquid densities were measured at these compositions in the temperature range from 243.15 to 280.15 K. The shape of the critical curves was studied at all compositions sudied.

Discussion

We developed an equation of state in the vapor region based on the present measurements using for it a functional form derived from the cubic equation of state:

$$P = RT[\ 1/(V-b) - a/(V(V+c)+d)].\tag{1}$$

Temperature dependences of the coefficients of Eq.(1) are following:

$$a = A_0(1 + A_1(1/\tau - 1) + A_2(1/\tau^2 - 1) + A_3(1/\tau^4 - 1));\quad b = const;$$

$$c = C_0 + C_1(1 - \tau) + C_2(1 - \tau)^2;\quad d = D_0 + D_1(1 - \tau).\tag{2}$$

The numerical constants in Eq.(2) are tabulated in Table 1 for pure components of the mixture. The mixing rules of the coefficients of Eq.(1) were given in the following equations:

$$a = \Sigma\Sigma\, X_i X_j (1 - K_{ij}^{\,a})(a_i a_j)^{0.5}; \quad b = \Sigma\Sigma\, X_i X_j (b_i b_j)^{0.5}$$

$$c = \Sigma\Sigma\, X_i X_j (1 - K_{ij}^{\,c})(c_i c_j)^{0.5}; \quad d = \Sigma\Sigma\, X_i X_j (1 + K_{ij}^{\,d})(d_i d_j)^{0.5} \tag{3}$$

The binary interaction parameters K_{ij} for the present system were determined to be:

$$K_{ij}^{\,a} = 0.305 + 0.1\,(X_2 - 0.36), [X_2 \leq 0.36]; \quad K_{ij}^{\,a} = 0.305 + 0.27\,(X_2 - 0.36), [X_2 > 0.36];$$

$$K_{ij}^{\,c} = 0.4; \quad K_{ij}^{\,d} = 0.4.$$

Deviation of the experimental data from those calculated by means of Eq.(1) did not exceed 0.6%.

Data [2] (P_s of composition X = 36 mol. % R116 in temperature range from 187 to 280 K) and our experimental VLE data of the mixture were used to determine parameters of the cubic equation of state (the equation used to calculate vapor - liquid equilibria):

$$P = RT[1/(V - b) - a/V(V + c)], \tag{4}$$

were a, b, c are coefficients determined from the conditions of vapor - liquid equilibria of the components of the mixture for each value of the temperature on the saturation line.

Using the same mixing rules (Eq.(3)), the binary interaction parameters K_{ij} were determined to be:

$$K_{ij}^{\,a} = 0.102 + 0.45X_2; \quad K_{ij}^{\,c} = 0.$$

The binary interaction parameters for the calculation of the saturated-liquid densities of mixture were determined to be:

$$K_{ij}^{\,a}=0.1,\ [X_2 \leq 0.44]; \quad K_{ij}^{\,a}=0.1+0.8(X_2-0.44), [X_2>0.44]; \quad K_{ij}^{\,c}=0.$$

Deviation of the measured bubble-point and dew-point pressures from values calculated using Eq.(2) did not exceed 1%. The maximum deviation between the measured saturated -liquid and saturated-vapor densities of mixture and those calculated from Eq.(2) was 0.4% and 1% respectively.

Table 1

Critical parameters and constants in Eqs.(2),(5),(6)

Coefficient	R23	R116
A_0	0.171583	0.257681
A_1	3.490379	$1.119119 \cdot 10^1$
A_2	-1.362514	-7.700742
A_3	$2.619432 \cdot 10^{-1}$	1.303123

Table 1 (continued)

Coefficient	R23	R116
B_0	-0.016	-0.009
C_0	0.073255	0.064110
C_1	$5.275804 \cdot 10^{-2}$	$-7.054309 \cdot 10^{-1}$
C_2	$2.717245 \cdot 10^{-1}$	$1.264610 \cdot 10^{-1}$
D_0	0.00852	0.02010
D_1	$-7.009538 \cdot 10^{-3}$	$1.042710 \cdot 10^{-1}$
E_1	7.17218	7.02955
E_2	5.2398	5.6778
E_3	2.64	2.64
F_1	1.7152	1.6495
F_2	0.3294	0.3261
T_c , K	299.0	293.0
P_c , MPa	4.8200	3.0386
ρ_c , $kg \cdot m^{-3}$	525.0	616.8

The thermal properties of the mixture on the vapor-liquid coexistence curve were calculated by the following equations:

$$\ln(p_c/p_s) = E_1 \ln(T_c/T) + E_2(\ln(T_c/T))^{E_3} \quad (5) \qquad \ln(\rho'/\rho_c) = F_1(\ln(T_c/T))^{F_2 f}, \qquad (6)$$

were $\quad f = 1 - 1.113(\ln(T_c/T))^{0.4}(\ln(\ln(T_c/T)))^{-1}$;

E_1, E_2, E_3, and F_1, F_2 - coefficients dependent on individual properties of substances.

The coefficients and critical parameters used for R23 and R116 are listed in Table 1.

Thermodynamic properties on the saturation line for composition of 36 mol.% R116 were calculated by using Eq.(4) and listed in Table 2.

The results for the critical parameters of the mixture can be represented by the following equations:

$$T_c = \sum t_i X^i; \qquad P_c = \sum P_i X^i; \qquad \rho_c = \sum \rho_i X^i. \qquad (7)$$

The coefficients of Eqs.(7) are listed in Table 3.

Table 2

Thermodynamic properties on the saturation line for composition X = 0.36

T K	P' MPa	P'' MPa	ρ' kgm^{-3}	ρ'' kgm^{-3}	h' kJkg^{-1}	h'' kJkg^{-1}	s' kJ(kg K)$^{-1}$	s'' kJ(kgK)$^{-1}$
180	0.0799	0.0785	1560.7	5.18	155.9	317.5	0.7594	1.6423
185	0.1044	0.1042	1540.5	6.73	168.1	320.3	0.8248	1.6339
190	0.1352	0.1352	1519.7	8.58	175.2	323.1	0.8603	1.6266
195	0.1734	0.1734	1498.5	10.81	180.4	325.6	0.8850	1.6193
200	0.2203	0.2203	1476.8	13.54	184.7	328.0	0.9046	1.6118
205	0.2773	0.2772	1454.5	16.82	188.4	330.2	0.9211	1.6039
210	0.3455	0.3455	1431.8	20.73	191.8	332.1	0.9358	1.5955
215	0.4263	0.4264	1408.3	25.36	194.8	333.7	0.9490	1.5864
220	0.5212	0.5213	1384.1	30.82	197.6	334.8	0.9609	1.5765
225	0.6316	0.6316	1358.9	37.21	200.1	335.5	0.9717	1.5655
230	0.7588	0.7588	1332.6	44.68	202.3	335.7	0.9814	1.5531
235	0.9045	0.9043	1304.8	53.37	204.2	335.1	0.9899	1.5390
240	1.0702	1.0698	1275.5	63.52	205.8	333.8	0.9970	1.5228
245	1.2577	1.2569	1244.2	75.37	207.0	331.5	1.0025	1.5038
250	1.4688	1.4675	1210.6	89.30	207.6	328.0	1.0061	1.4814
255	1.7056	1.7037	1174.4	105.79	207.5	323.0	1.0072	1.4546
260	1.9703	1.9678	1135.1	125.52	206.4	316.1	1.0052	1.4220
265	2.2654	2.2622	1091.9	149.52	204.2	306.6	0.9992	1.3817
270	2.5936	2.5899	1043.9	179.38	200.3	293.5	0.9876	1.3305
275	2.9582	2.9545	989.8	217.77	193.9	275.1	0.9679	1.2631
280	3.3634	3.3607	928.2	269.62	183.7	248.3	0.9355	1.1695
285	3.7230	3.6539	836.8	293.18	169.7	236.8	0.8921	1.1339

Table 3

Parameters used in Eqs. (7)

i	t_i	P_i	ρ_i
0	299.06	48.086	525.06
1	-54.03869	-23.65859	147.6902
2	63.49612	6.05004	-56.04627
3	-15.40773	-	-

Conclusions

Our investigation allows to infer that the mixture forms positive azeotrope and that azeotropic concentration changes its value from x=0.39 at 180 K to x=0.33 at 285 K.

References

1. Zhelezny, Yu.V. Semenyuk and Yu.A. Chernyak, Proc. 13th European Conf. on Thermoph. Prop., (Lisbon, Portugal, 1993), pp. 361-362.

2. Vladimirov, Yu.F. Shvets, Pressure of the saturation vapor of R218,R329 and azeotropic mixture R116/R23. Thermoph. Prop. of Substances and Materials, **28:** 28   (1989). (in Russian).
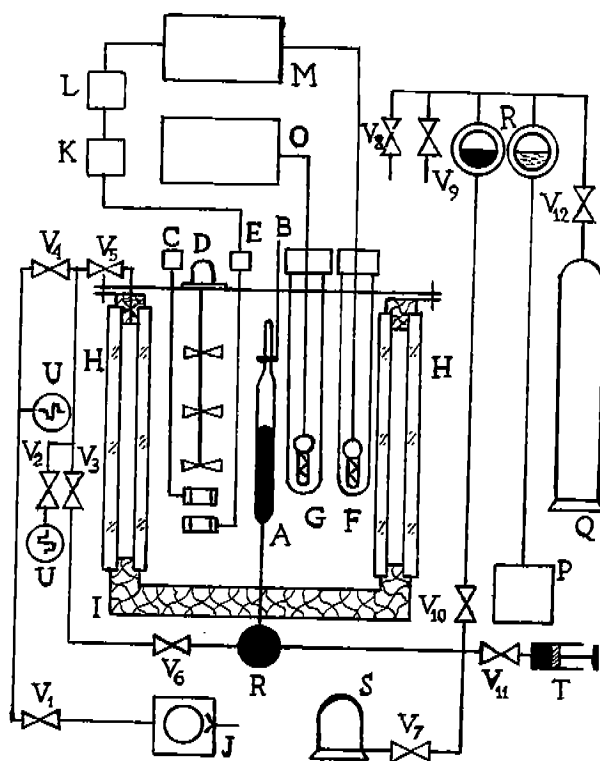
Experimental apparatus

Fig.

A, optical cell; B, magnetic stirrer; C, main heater; D, stirrer; E, subheater; F,G, platinum resistance termometres; H, windows; I, thermostat; J, vacuum pamp; K,thyristor amplifier; L, PID controller; M, thermometer bridge; O, potentiometer; P, dead-weigh pressure gauge; Q, nitrogen gas; R, separators; S, Hg-cylinder; T, precise volume controller; U, vacuum gauge; V_1-V_{12}, valves.

PERFORMANCE OPTIMIZATION OF A LARDER TYPE REFRIGERATOR UNIT USING COMPUTER AIDED ANALYSIS TOOLS

Engin Dirik, Harun İz, Cezmi Aydın
ARCELİK A.Ş,. Research and Development Center,
Tuzla 81719, İstanbul, TURKEY

ABSTRACT

This paper describes the utilisation of computer aided analysis tools in the design and performance optimisation process of domestic refrigerators. A larder type table-top refrigerator unit is considered in the present study. In the first phase of the project, the existing refrigerator using CFC-12 as a working fluid was converted into a prototype with environmental benign refrigerant isobutane, R600a. The conversion process involved compressor stroke volume and refrigerant charge adjustments to achieve the same cooling performance. In the second phase, in-house developed refrigeration cycle simulation code and commercial Computational Fluid Dynamics (CFD) packages were used for the optimisation with respect to energy consumption. Design parameters of the main components of the refrigeration circuit, namely compressor, condenser, evaporator and capillary tube-suction line intercooler assembly were modified based on the results of computer simulations. Three prototypes were subsequently built and tested under standard climatic conditions. Redesigned unit has been found to have significantly lower energy consumption compared with the existing refrigerator.

INTRODUCTION

The ongoing phaseout process of ozone depleting clorofluorocarbons (CFCs) and the increasing emphasis on global warming considerations which demand the production of more energy efficient appliances have been forcing domestic refrigerator manufacturers for the design changes and improvements on their existing product lines. To help to facilitate this need, a flexible component based computer simulation package for the performance prediction of the household refrigerator/freezer units has been developed. Extensive use of this in-house developed analysis capacity is being made in the product development environment. Commercial CFD packages are also being used routinely to support the refrigerator design process.

In this study, utilisation of the established capacity is described for the redesign case of a larder type refrigerator unit. The redesign objective was twofold: (i) conversion to an environmentally friendly hydrocarbon refrigerant, R600a from CFC-12 and (ii) improvement in energy consumption.

Since the beginning of 1990's, appliance manufacturers in Europe have started using hydrocarbons refrigerants in domestic refrigerators. Hydrocarbons are environmentally safe substances since they have no ozone depletion and negligible global warming potential. Among their advantages, superior transport properties (high thermal conductivity and lower viscosity) , requirement for lower amount of charge compared with CFC and HFC type refrigerants, solubility in traditionally used lubricant mineral oil can be stated. These advantages are so attractive for refrigeration system designers and the people who care for nature that the efforts spent for the design of a risk-free system are easily justified. Although it requires some design changes in the cooling circuit components, isobutane became the choice of domestic refrigeration producers among other hydrocarbon refrigerants. The reason for its selection is that it allows the compressor to operate under less loads thus causing more reliable and a quieter system.

In the first part of the paper, the establish simulation capabilities are reviewed. The refrigerant replacement and the energy optimisation methodology followed in the redesign process are presented in the remainder of the paper after a brief description of the existing refrigerator unit.

REFRIGERATION CYCLE SIMULATION PACKAGE: REFSIM

The mathematical models for the main components of the vapour compression based refrigeration circuitry, namely compressor, condenser, capillary tube-suction line intercooler assembly and evaporator were developed from the fundamental conservation principles. Special test facilities were designed and fabricated for the model validation studies of the individual components. The component models were subsequently incorporated into a robust and efficient computer algorithm for the performance simulation of entire refrigerator unit under the steady-state regime. The steady-state simulation model were then extended to include on/off working conditions by adapting the cycle-average strategy. The final software product were verified using the experimental measurements taken on specially intstrumented refrigerator units. The component models are described briefly in the following subsections.

Compressor Model: The biquadratic curve fits as a function of condensing and evaporating temperatures are obtained from the compressor map data and used for both compressor mass flow rate and power predictions. The compressor discharge temperature under different operating conditions is determined from the first-law energy balance which relates input power, heat rejection from the canister and enthalpy change of refrigerant across the compressor. The rate of heat loss from the compressor canister is calculated in terms of the convection heat transfer equation. This equation is based on the refrigerant discharge temperature for simplicity. The overall conductance value of the compressor is estimated from the test data measured at the standard rating point.

Condenser Model: A simple model based on the measured values of air side heat transfer coefficient is established for the tube-and-wire type condenser unit. Experiments were conducted for a number of relevant geometric configurations and wide range of operating temperatures by circulating hot water inside the condenser tubes. The measured values of natural heat transfer coefficients are correlated in terms of temperature difference between the condenser and the ambient air for each unit tested. The relative position and the inclination of the condenser unit were changed systematically to study effects of these parameters and determine the optimum configuration. The thermal efficiency of condenser wires were calculated from the standard expressions of fins given in common literature. The tube side heat transfer coefficient for the condensing refrigerant is obtained from the correlations given in [1].

Capillary Tube-Suction Line Heat Exchanger Assembly Model: The REFSIM package includes a comprehensive and a rigorous numerical model for the performance prediction of the capillary tube expansion device. The present numerical model was intended to account for the effects of suction line cooling on the performance characteristics of capillary tubes in order to capture the true system performance [2]. The governing equations for steady one-dimensional homogeneous equilibrium two-phase flow through the capillary tube are obtained by applying basic conservation principles to differential control volumes. The subsequent numerical solution is facilitated by transforming these equations into a more convenient form in terms of numerical integration. The transformed equations along with the energy equation of for steady one-dimensional gas flow through the suction line forms an initial value problem. Forth order Runge-Kutta algorithm is used to march advance the solution along the capillary tube length until the critical conditions is reached. Mass flow rate is continuously adjusted until the calculated tube length equals to the prescribed tube length. Additional iteration loop is required on suction line exit temperature to match the calculated suction inlet temperature to the prescribed conditions at the evaporator outlet.

Evaporator Model: The evaporating refrigerant flowing inside the tubes exchanges heat with the cabinet air. The mathematical model for the tube-on-sheet type cold wall evaporator is formed in a way similar to the condenser unit. A boundary layer type flow exists in the vicinity of cold evaporator surface inside the cabinet. The air side heat transfer coefficient in the boundary layer were determined from the numerical experiments conducted on full cabinet geometry. The details of the CFD studies performed in the present work is discussed in the following section. The calculated values also includes the effects of surface-to-surface radiation heat exchange which takes place inside the cabinet enclosure. The refrigerant side heat transfer coefficients were obtained from the correlations given in [3]. The thermal resistances due to heat conduction and the thermal contacts of the tube-on-sheet assembly were estimated by using the experimental data obtained from the existing refrigerator unit.